Electrosynthesis of oligo(methoxyl pyrene) for turn-on fluorescence detection of volatile aromatic compounds†

Yuanwei Gao, Hua Bai* and Gaoquan Shi*

Received 27th November 2009, Accepted 26th January 2010
First published as an Advance Article on the web 22nd February 2010
DOI: 10.1039/b924992c

A highly fluorescent conjugated oligomer, oligo(1-methoxyl pyrene) (OMOPr), was synthesized *via* electrochemical polymerization and its structure was studied by UV-vis spectroscopy, MALDI-TOF mass spectroscopy and *ab initio* calculation. The organic solutions of OMOPr emit strong blue lights and show solvatochromic effect, while these fluorescence emissions are quenched upon chain aggregation in its dry films. On the basis of these phenomena, a turn-on fluorescence sensor was fabricated and it can be used for detecting volatile aromatic compounds (VACs).

Introduction

Conjugated polymers (CPs) have attracted wide interest due to their promising applications in organic electronics, solar cells, actuators, sensors and biotechnologies.[1] Among these polymers, polypyrene or oligopyrene (OPr) and its derivatives have unique properties including high crystallinity and blue or multicolored fluorescence with high quantum yields.[2] Therefore, they have various applications in fluorescence sensing.[3] For example, OPr has been used as a probing molecule for detecting nitroaromatic compounds both in atmosphere and aqueous media.[3a,3b] This is mainly due to the large conjugated pyrenyl rings of OPr chain backbones that have strong affinity with aromatic molecules.

It is known that pyrene can be electrochemically polymerized into OPr with 2–10 repeat units.[2a,2b,2d] However, only OPr with short chain lengths (2–6 repeat units) are soluble,[3a] due to its rigid chain backbones and the lack of graft chains. Therefore, several derivatives of OPr such as oligo(1-pyrenebutyric acid) and its ester were synthesized.[3b–d,4] These oliogmers are soluble in water because of their negatively or positively charged side groups.[3b–d,5] Nitryl and phenyl substituted OPr have also been synthesized *via* electrochemical and chemical polymerizations.[6] However, alkoxyl, an important substituent usually used to adjust the band gaps and solubility of CPs,[7] has not yet been introduced into OPr. As an electron-rich functional group, alkoxyl can increase the electron densities of CP backbones and lower the band gaps of the corresponding polymers.[8] Therefore, it is expected that alkoxyl substituted OPr has unique optical properties for sensing applications.

In this article, we report the synthesis of oligo(methoxy pyrene) (OMOPr) through electrochemical polymerization (Scheme 1). OMOPr is soluble in common solvents such as tetrahydrofuran (THF) and chloroform, and its solution is highly fluorescent. Furthermore, the emission of OMOPr showed a solvatochromic effect in various organic solvents. However, the solid film of OMOPr exhibited weak emission and its fluorescence could be strongly enhanced (fluorescence "turn-on") upon exposing to the vapors of volatile aromatic compounds (VACs). On the basis of these phenomena, OMOPr films were utilized as sensors to detect VAC vapors.

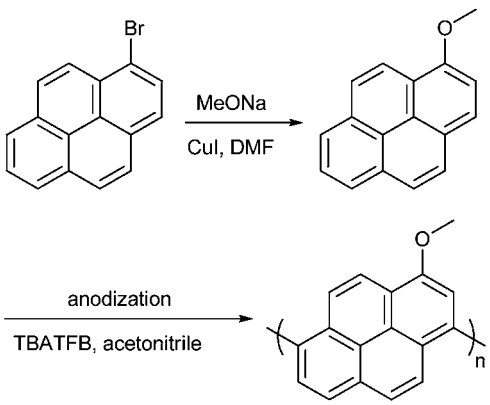

Scheme 1 Synthesis route of OMOPr.

Results and discussion

Synthesis and electrochemical properties of OMOPr

The monomer, MOPr, was synthesized according to a published procedure (Scheme 1).[9] It was obtained in high yield and well purified for electrochemical polymerization (Fig. S1†). Fig. 1 shows the cyclic voltammograms (CV) of 0.02 M MOPr in acetonitrile containing 0.1 M TBATFB. Each CV cycle has a pair of redox waves attributed to the redox reaction of MOPr ↔ $MOPr^{\bullet+}$ in the potential scale of 0.2 to 1.0 V (*vs.* Ag/Ag^{+}). However, the currents of both waves did not increase appreciably during successive CV scans, implying that only a trace amount of product was deposited onto the working electrode. Thus, it is reasonable to conclude that the electrochemically generated $MOPr^{\bullet+}$ radical cations were mostly reduced to neutral monomers again during the opposite CV scans. This process was also reflected by the color change of the electrolyte: when MOPr was oxidized at high potentials, the color of the solution close to the

Key Laboratory of Bioorganic Phosphorus Chemistry & Chemical Biology, Department of Chemistry, Tsinghua University, Beijing, 100084, People's Republic of China. E-mail: baihua00@mails.tsinghua.edu.cn; gshi@tsinghua.edu.cn

† Electronic supplementary information (ESI) available: NMR and additional fluorescence spectra. See DOI: 10.1039/b924992c

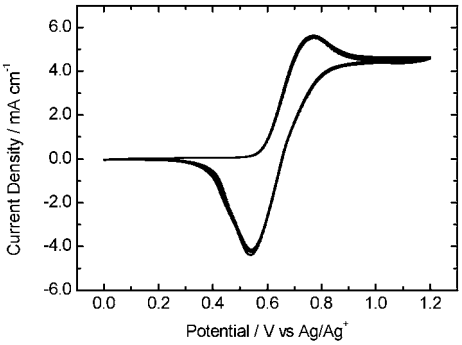

Fig. 1 Cyclic voltammograms of 0.02 M MOPr in acetonitrile containing 0.1 M TBATFB at a potential scan rate of 50 mV s^{-1}.

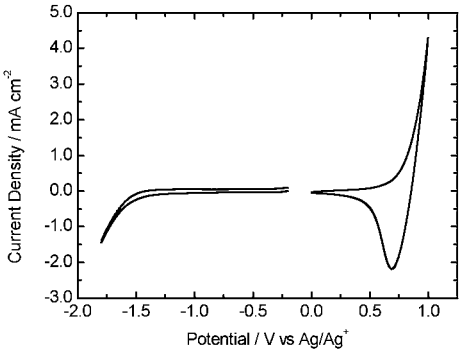

Fig. 3 Cyclic voltammogram of an OMOPr film in acetonitrile containing 0.1 M TBATFB at a potential scan rate of 50 mV s^{-1}.

surface of working electrode turned dark, while this color faded during the opposite CV scan. This phenomenon reveals that the polymerization of MOPr is a slow process with low current efficiency. Considering the well-accepted polymerization mechanism of aromatic monomers, involving the coupling of two radical cations, the slow polymerization of MOPr is mainly due to the low reactivity of MOPr$^{\bullet+}$.[10] The large π conjugated system of MOPr stabilized its radical cations and reduced the possibility of coupling reactions.

MOPr has been successfully polymerized potentiostatically at 0.75 V. During this process, the reduction of MOPr$^{\bullet+}$ species was prevented and the coupling reaction was accelerated by increasing the concentration of the radical cations. After electrolysis for 24 h, a brown solid was deposited on the working electrode surface and also there was some product precipitated onto the bottom of electrochemical cell. These solids were collected and treated with hydrazine to reduce any possible cation species. After careful purification, neutral OMOPr as a khaki powder was obtained. It is soluble in common solvents such as chloroform and THF, and its degree of polymerization was measured by MALDI-TOF mass spectroscopy to be 2–6 (Fig. 2).

The cyclic voltammogram of an OMOPr thin film in acetonitrile containing 0.1 M TBATFB is illustrated in Fig. 3. It is clear from this figure that the oxidation and reduction potentials of OMOPr are at 0.75 V and −1.54 V *vs.* Ag/Ag^{+}, respectively. The oxidation current increases sharply at the potentials higher than 1.2 V *vs.* Ag/Ag^{+} due to over-oxidation of the oligomer. As a result, the electrochemical activity of the oligomer gradually disappeared in successive CV cycles. The reduction of OMOPr is irreversible and the corresponding wave current also decreased gradually in the following CV scans. These results reflect that OMOPr is an electron donor, mainly due to the introduction of the electron-rich alkoxyl substituent.

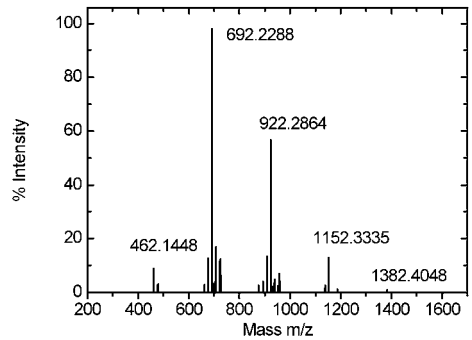

Fig. 2 MALDI-TOF mass spectrum of OMOPr.

Theoretical studies of OMOPr

To study the molecular structure and the polymerization process of OMOPr, we performed *ab initio* calculations using Gaussian software.[11] First, the dimerization reaction was considered. According to the well-accepted mechanism, the first step of electrochemical polymerization of an aromatic compound is oxidation of the monomers to produce radical cations. Then, a dimer is formed through coupling two radical cations and successive removal of two protons.[10b] Since the MOPr$^{\bullet+}$ radical cation has several available positions for the coupling reaction, it is necessary to confirm which position(s) is (are) the most favorable one(s) for the formation of dimers. According to the literature, the distribution of spin density in the radical cation can be used to predict the connect type of the coupling reaction: the coupling reaction occurs at the atoms with high spin densities.[12] We used density functional theory (DFT) at B3LYP/6-31G(d) level for calculating the atomic spin density of each carbon atom and the results are demonstrated in Scheme 2. The carbon atoms at positions 6 and 8 of the monomer are most reactive for coupling, position 6 being slightly more favorable. Therefore, the dimers were most likely formed through 6–6′, 6–8′ or 8–8′ coupling, and 6–6′ coupling is dominant. These results are consistent with the reactivity of pyrene whose positions 1, 3, 6 and 8 are the active sites.[13] Besides, position 5 of MOPr also has a relatively high spin density, which is quite different from that of pyrene molecule (Fig. S2†), indicating that the alkoxyl group has a remarkable influence on the electron distribution in pyrenyl ring.

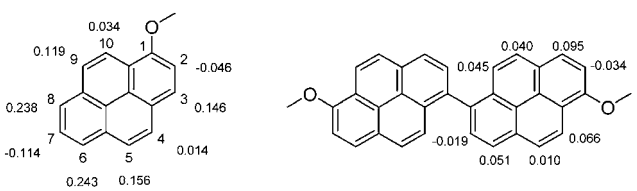

Scheme 2 Calculated spin density of MOPr$^{\bullet+}$ and MOPr$_2^{\bullet+}$.

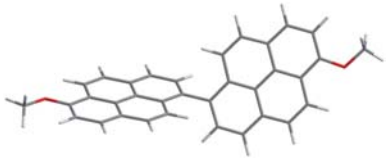

Fig. 4 Calculated molecular structure of $MOPr_2$.

Second, the spin densities on the 6,6′-dimer radical cation ($MOPr_2^{\bullet+}$) were calculated, and the results revealed that its position 3 is the most reactive site. However, the spin density values in the dimer radical cation are much lower than those in the monomer radical cation, because an electron is delocalized in an expanded conjugated structure. This explains why it is hard to obtain poly(methoxyl pyrene) with high molecular weight: the delocalization effect decreases the reactivity of the radical cationic oligomers and also reduces the possibility of chain elongation.

The optimized structure (B3LYP/6-31G*) of $MOPr_2$ is shown in Fig. 4. According to the calculation results, the dimer has a large dihedral angel of 69.8° between two neighboring pyrenyl planes due to the repulsion of hydrogen atoms at positions 5 and 7. This value is close to that of oligopyrene.[3a] We further calculated the potential energy curve of OMOPr during the rotation of the C6–C6′ bond, which can be used to estimate the rigidity of the OMOPr backbone, and the results show that the rotation of C6–C6′ is rather difficult (Fig. S3†).[14] An energy barrier of 8.7 kJ mol^{-1} is needed to change the dihedral angel from 70° to 45°, and 76.3 kJ mol^{-1} is required to change the stable conformation into a fully co-planar structure. These values are much higher than those of polythiophenes.[14a] Therefore, the OMOPr chain is rigid and the torsional angle of neighboring pyrenyl rings is limited in a narrow range.

Spectral properties of OMOPr

Fig. 5 demonstrates the UV-visible spectra of the THF solutions of MOPr and OMOPr. The spectrum of MOPr is different from that of pyrene,[2a] because the conjugation of the oxygen atom altered the energy level of the pyrenyl ring and the oscillator strength of each electron transition. In comparison with that of MOPr, the absorption maximum of OMOPr solution red-shifted from 346.5 to 369 nm, indicating the enlargement of the conjugated system. From the onset of the absorption spectrum, the energy gap of OMOPr was calculated to be 2.8 eV. Furthermore, it is noted that the vibration structures can be observed from the absorption spectrum of OMOPr solution even at low concentration. This is mainly due to the OMOPr chains being rather stiff, leading to very limited conformations even in dilute THF solutions.[15]

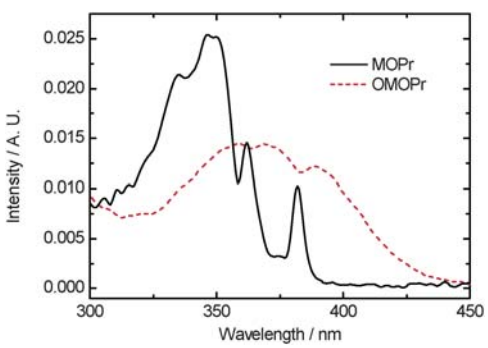

Fig. 5 UV-visible spectra of 1.34×10^{-6} M THF solutions of MOPr and OMOPr.

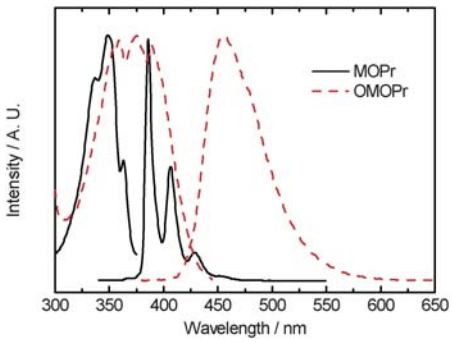

Fig. 6 Normalized excitation and fluorescence spectra of 2×10^{-5} M THF solutions of MOPr and OMOPr.

The OMOPr solution can emit bright blue fluorescence light with a fluorescence quantum yield (ϕ_f) of 0.77, while the ϕ_f of MOPr is only 0.61. The fluorescence excitation and emission spectra of MOPr and OMOPr are shown in Fig. 6. There is a large stokes shift between the excitation and emission bands of MOPr, indicating the structure of MOPr in the excited state differs from that in ground state. This is possibly due to the conjugation of oxygen atom or solvation effect in the excited state. The emission maximum of OMOPr (456 nm) showed a 70 nm red-shift compared with that of MOPr (386 nm). No vibration structures were found from the emission bands of OMOPr, reflecting that the oligomer chain in excited state has diverse conformations.[15]

Fig. 7 shows the normalized UV-visible and fluorescence spectra of 5×10^{-5} M OMOPr in seven different solvents (the original emission spectra are shown in Fig. S4†). The overall

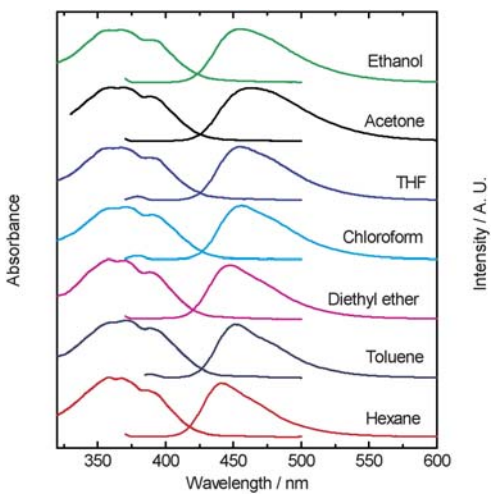

Fig. 7 Normalized UV-visible and fluorescence spectra of 5×10^{-5} M OMOPr in seven different solvents.

features of the absorption spectra are almost the same, indicating the conformation of the OMOPr molecule in the ground state is fixed due to the high rotational energy barrier. However, the fluorescence spectra exhibit an obvious solvatochromic effect. For example, the emission maximum of OMOPr in hexane is at 441 nm while that in acetone is at 464 nm. The solvent-induced shift in emission band can be explained as the result of the solvent polarity change, which alters the energy levels of the excited OMOPr.[16] Since excited molecules usually exhibit a larger dipole moment, solvents with large polarity can effectively lower the energy, leading to a red-shift of the emission band. It is also clear from Fig. 7 that ethanol and diethyl ether, two polar solvents, do not lower the emission energy of excited OMOPr dramatically as expected. This is possibly due to these solvents having a much stronger interactions with methoxyl substituents than those with pyrenyl rings of OMOPr chains.

Although the OMOPr solution is fluorescent, the emission of its solid film is weak. To investigate the fluorescence quenching process, the fluorescence spectra of OMOPr in different THF–water mixed solvents were recorded. As shown in Fig. 8, with the addition of water to a THF solution, the emission band of OMOPr shifted to longer wavelengths. This phenomenon is attributed to the polarity increase of the solvent lowered the energy of OMOPr in excited state. However, when the water content was increased to 70% (by volume), the fluorescence intensity decreased dramatically, due to the aggregation of OMOPr chains in their poor solvent. Further increases to the content of water led to an extensive quenching of the emission. In the solvent containing 80% or 90% water, the emission at ~460 nm disappeared while a new weak emission band at ~600 nm emerged (inset of Fig. 8). Since the excitation spectrum monitored at 600 nm is the same as that detected at 460 nm (Fig. S5†), it is reasonable to attribute this new emission to excimer species. The spectral results described above indicate that the fluorescence quenching of the OMOPr film resulted from its chain aggregation.

Fluorescence sensing

Detection of volatile organic compounds (VOCs) is of special importance because their vapors are both toxic and explosive, and colorimetric sensors based on conjugated polymers were reported to be able to detect and distinguish VOC.[17] These

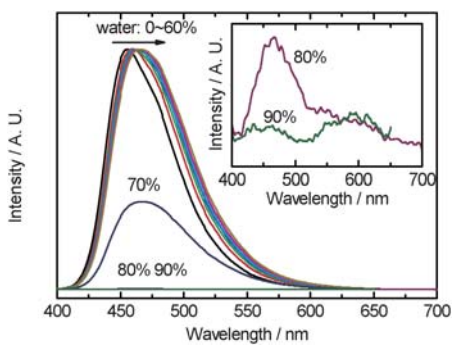

Fig. 8 Fluorescence spectra of 5×10^{-5} M OMOPr in mixed solvents of THF and water. Inset: fluorescence spectrum of OMOPr in mixed solvent containing 80% or 90% water (by volume).

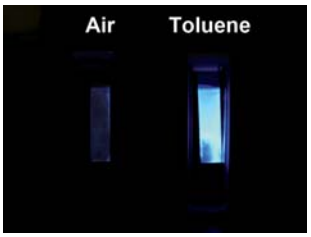

Fig. 9 The images of an OMOPr test paper in dry air or in toluene vapor upon excitation with a 365-nm UV light.

sensors undergo color changes upon contact with VOCs. On the other hand, fluorimetry is considered to be a sensitive technique for detecting various analytes, and a turn-on process is favorable for fluorescence colorimetric sensing. In this case, the detection of small signal increases from a very low initial level is easier, and the measurement of the emission band shift will not be interfered with by the background signal.[18] On the basis of the solvatochromic effect and the unique chain structure of OMOPr film, a "turn-on" fluorescence sensor was fabricated for detecting volatile aromatic compounds (VACs), a family of VOCs. As shown in Fig. 9, a fluorimetric test paper was prepared by soaking a filter paper with OMOPr solution and then dried in air. The dry test paper showed weak emission under irradiation with a 365-nm UV light (Fig. 9, left). However, the fluorescence

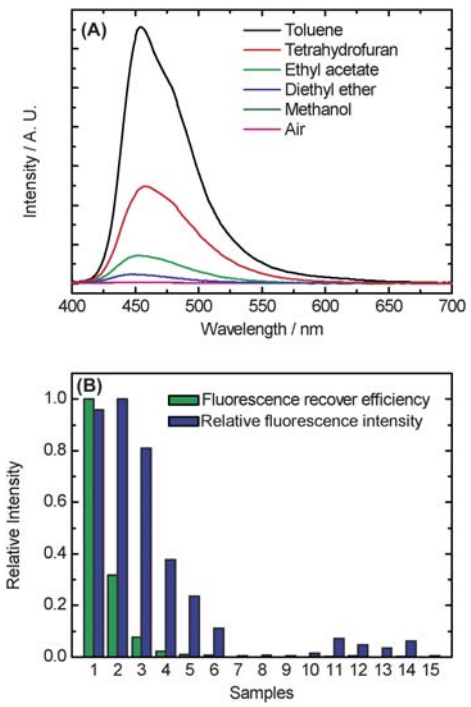

Fig. 10 (A) Fluorescence spectra of an OMOPr thin film after exposure to air or various saturated organic vapors. (B) Relative fluorescence intensity of an OMOPr thin film in different saturated organic vapors and relative fluorescence recovery efficiencies (the ratio of fluorescence intensity to saturated vapor pressure) of these vapors. Samples: 1, xylene; 2, toluene; 3, benzene; 4, tetrahydrofuran; 5, chloroform; 6, ethyl acetate; 7, methanol; 8, ethanol; 9, *iso*-propanol; 10, hexane; 11, dichloromethane; 12, carbon tetrachloride; 13, diethyl ether; 14, acetone; 15, acetonitrile.

intensity of the test paper increased dramatically and rapidly after contacting with a saturated vapor of toluene, a typical VAC (Fig. 9, right). This is due to solvation and dissociation of OMOPr aggregates by adsorbed toluene molecules. Therefore, this test paper is a naked-eye sensor for detecting toluene vapor.

As mentioned above, the emission band features of OMOPr solutions strongly depend on their solvent properties. Therefore, it is possible to distinguish various VOCs based on the fluorescence spectral changes of OMOPr films upon exposure to their vapors. Fig. 10A represents the fluorescence spectra of an OMOPr film in air and those in the vapors of five typical VOCs. Fig. 10B depicts the fluorescence intensities of an OMOPr film in 15 VOC vapors. To evaluate the fluorescence enhancing ability of each solvent vapor, fluorescence enhancing efficiency (η_f) is defined as the ratio of fluorescence intensity to saturated vapor pressure of a given organic solvent.[19] One can see from Fig. 10 that the VACs including xylene, toluene and benzene exhibit the highest η_f values. Therefore, we can simply distinguish VACs vapors from the other organic vapors. Since the fluorescence quantum yield of OMOPr in these solvents varies only in a relative small range (0.5–1) according to the band areas of the fluorescence spectra (Fig. S4†), the fluorescence intensity of solvated OMOPr film must be governed by the amounts of fluorescent isolated OMOPr molecules. Aromatic molecules have strong π–π interactions with the pyrenyl rings of OMOPr, facilitating their molecular adsorptions in the film and the dissociation of OMOPr aggregates. Therefore, the selectivity of OMOPr film towards VACs vapors relies on its large aromatic pyrenyl rings, which provide selective affinity to VACs.

Experimental

Materials

1-Bromopyrene was purchased from Pacifichem (China), and tetrabutylammonium tetrafluoroborate (TBATFB) was bought from Aldrich. All the other solvents and chemicals were the products of Beijing Chemical Plant. Acetonitrile and tetrahydrofuran (THF) were dried by refluxing with calcium chloride and sodium, respectively, and distilled before use. Other reagents were used as received without further purification.

Synthesis of OMOPr

The synthesis route of OMOPr is depicted in Scheme 1. 1-Methoxyl pyrene (MOPr) was synthesized according to the literature,[9] and its structure and purity were examined by NMR (Fig. S1†). OMOPr was prepared by electrochemical polymerization. In a typical experiment, an acetonitrile solution containing 0.02 M MOPr and 0.1 M TBATFB was used as the electrolyte. The electrolyte was deoxygenated by bubbling nitrogen gas and a slight over-pressure was maintained during electrosynthesis. A conductive indium tin oxide glass (ITO, 1 cm × 1 cm) and a platinum sheet (1 cm × 1 cm) were used as the working and counter electrodes, respectively. All the potentials were referred to an Ag/Ag^+ electrode. OMOPr was polymerized potentiostatically at voltage of 0.75 V for 24 h. After the polymerization, the dark brown solid was collected from the working electrode, and stirred in hydrazine solution in ethanol for 9 h. The reduced OMOPr was then filtered and purified using a silica gel column (eluant = 1 : 1 hexane : dichloromethane). Finally, the oligomer was further purified by precipitating from its concentrated dichloromethane solution with hexane, and dried in vacuum.

Fluorescence measurement

The fluorescence quantum yields (ϕ_f) of MOPr and OMOPr were measured by using quinoline sulfate in 0.1 M H_2SO_4 as the reference ($\phi_{f350} = 0.577$, $\phi_{f365} = 0.53$).[20] For the sensing test, the thin film of OMOPr was prepared by spin-coating its THF solution (5×10^{-5} M) onto a quartz slice at a spin rate of 400 rpm. The fluorescence spectrum of the film was measured with the OMOPr coated quartz slice placed in a conventional fluorescence cuvette. To measure the fluorescence spectra of the film in a given organic vapor, several drops of the solvent was dropped onto the bottom of the cuvette. Then, the quartz slice with OMOPr film was inserted in the sealed cuvette to contact with the saturated vapor. The fluorescence spectrum of OMOPr in the vapor was recorded as the spectral intensity became stable.

Instruments and characterization

The electrochemical experiments were performed on a 440A (CHI, USA) potentiostat under computer control. Ultraviolet-visible (UV-vis) spectra were recorded on a U-3010 (Hitachi, Japan) UV-visible spectrometer, and the fluorescence spectra were measured on a LS-55 (Perkin Elmer, USA) spectrometer. ^{1}H-NMR spectroscopy was carried out on a JNM-ECA300 NMR spectrometer (JOEL, Japan). MALDI-TOF mass spectrometry was carried out by using a BIFLEXIII mass spectrometer (Bruker, USA).

Conclusions

In summary, we have synthesized OMOPr by facile electrochemical polymerization. Theoretical study indicates that the polymerization occurs at positions 6 and 8 of the monomer. The bond rotation between adjacent pyrenyl rings of an OMOPr chain is difficult due to a high energy barrier. OMOPr solutions have high fluorescence quantum yields, but its film is non-emissive. The fluorescence of an OMOPr thin film can be enhanced upon exposure to organic vapors, especially, to aromatic solvent vapors. The selectivity towards aromatic solvents is attributed to the strong π–π interaction between the pyrenyl rings of OMOPr and the aromatic solvent molecules.

Acknowledgements

This work was supported by the National Natural Science Foundation of China (50533030, 50873052 and 20774056) and China Postdoctoral Science Foundation (20090460027).

Notes and references

1 (*a*) A. C. Grimsdale, K. L. Chan, R. E. Martin, P. G. Jokisz and A. B. Holmes, *Chem. Rev.*, 2009, **109**, 897–1091; (*b*) S. Günes, H. Neugebauer and N. S. Sariciftci, *Chem. Rev.*, 2007, **107**, 1324–1338; (*c*) C. Winder and N. S. Sariciftci, *J. Mater. Chem.*, 2004, **14**, 1077–1086; (*d*) H. Bai and G. Q. Shi, *Sensors*, 2007, **7**, 267–307; (*e*) C. Li, H. Bai and G. Q. Shi, *Chem. Soc. Rev.*, 2009, **38**, 2397–2409; (*f*) B. Liu and G. C. Bazan, *Chem. Mater.*, 2004, **16**,

4467–4476; (*g*) S. W. Thomas, G. D. Joly and T. M. Swager, *Chem. Rev.*, 2007, **107**, 1339–1386; (*h*) L. Zhao, L. Tong, C. Li, Z. Z. Gu and G. Q. Shi, *J. Mater. Chem.*, 2009, **19**, 1653–1658.
2 (*a*) G. W. Lu, L. T. Qu and G. Q. Shi, *Electrochim. Acta*, 2005, **51**, 340–346; (*b*) L. T. Qu and G. Q. Shi, *Chem. Commun.*, 2004, 2800–2801; (*c*) T. M. Figueira-Duarte, S. C. Simon, M. Wagner, S. I. Drtezhinin, K. A. Zachariasse and K. Mullen, *Angew. Chem., Int. Ed.*, 2008, **47**, 10175–10178; (*d*) G. W. Lu and G. Q. Shi, *J. Electroanal. Chem.*, 2006, **586**, 154–160.
3 (*a*) H. Bai, C. Li and G. Q. Shi, *Sens. Actuators, B*, 2008, **130**, 777–782; (*b*) Y. Q. Chen, H. Bai, Q. Chen, C. Li and G. Q. Shi, *Sens. Actuators, B*, 2009, **138**, 563–571; (*c*) Y. Q. Chen, H. Bai, W. J. Hong and G. Q. Shi, *Analyst*, 2009, **134**, 2081–2086; (*d*) Y. Q. Chen and G. Q. Shi, *Sensors*, 2009, **9**, 4164–4177.
4 X. F. Wu and G. Q. Shi, *J. Mater. Chem.*, 2005, **15**, 1833–1837.
5 L. Zhao, T. Ma, H. Bai, G. W. Lu, C. Li and G. Q. Shi, *Langmuir*, 2008, **24**, 4380–4387.
6 (*a*) B. Y. Lu, J. K. Xu, C. L. Fan, F. X. Jiang and H. M. Miao, *Electrochim. Acta*, 2008, **54**, 334–340; (*b*) S. I. Kawano, C. Yang, M. Ribas, S. Baluschev, M. Baumgarten and K. Mullen, *Macromolecules*, 2008, **41**, 7933–7937.
7 (*a*) J. Roncali, *Chem. Rev.*, 1992, **92**, 711–738; (*b*) S. Pfeiffer and H. H. Horhold, *Macromol. Chem. Phys.*, 1999, **200**, 1870–1878.
8 J. Roncali, *Chem. Rev.*, 1997, **97**, 173–206.
9 P. Demerseman, J. Einhorn, J. F. Gourvest and R. Royér, *J. Heterocycl. Chem.*, 1985, **22**, 39–43.
10 (*a*) J. Bargon, S. Mohmand and R. J. Waltman, *IBM J. Res. Dev.*, 1983, **27**, 330–341; (*b*) G. Sabouraud, S. Sadki and N. Brodie, *Chem. Soc. Rev.*, 2000, **29**, 283–293.
11 M. J. Frisch, G. W. Trucks, H. B. Schlegel, G. E. Scuseria, M. A. Robb, J. R. Cheeseman, V. G. Zakrzewski, J. A. Montgomery, Jr., R. E. Stratmann, J. C. Burant, S. Dapprich, J. M. Millam, A. D. Daniels, K. N. Kudin, M. C. Strain, O. Farkas, J. Tomasi, V. Barone, M. Cossi, R. Cammi, B. Mennucci, C. Pomelli, C. Adamo, S. Clifford, J. Ochterski, G. A. Petersson, P. Y. Ayala, Q. Cui, K. Morokuma, D. K. Malick, A. D. Rabuck, K. Raghavachari, J. B. Foresman, J. Cioslowski, J. V. Ortiz, B. B. Stefanov, G. Liu, A. Liashenko, P. Piskorz, I. Komaromi, R. Gomperts, R. L. Martin, D. J. Fox, T. Keith, M. A. Al-Laham, C. Y. Peng, A. Nanayakkara, C. Gonzalez, M. Challacombe, P. M. W. Gill, B. G. Johnson, W. Chen, M. W. Wong, J. L. Andres, M. Head-Gordon, E. S. Replogle and J. A. Pople, *Gaussian 98*, Revision A.9, Gaussian, Inc., Pittsburgh PA, 1998.
12 (*a*) S. Ando and M. Ueda, *Synth. Met.*, 2002, **129**, 207–213; (*b*) P. Audebert, J. M. Catel, G. Le Coustumer, V. Duchenet and P. Hapiot, *J. Phys. Chem. B*, 1998, **102**, 8661–8669.
13 H. Vollmann, H. Becker, M. Corell and H. Streeck, *Justus Liebigs Ann. Chem.*, 1937, **531**, 1–159.
14 (*a*) N. Di Césare, M. Belletête, G. Durocher and M. Leclerc, *Chem. Phys. Lett.*, 1997, **275**, 533–539; (*b*) N. Di Césare, M. Belletête, M. Leclerc and G. Durocher, *Synth. Met.*, 1998, **94**, 291–298; (*c*) G. A. Diaz-Quijada, N. Weinberg, S. Holdcroft and B. M. Pinto, *J. Phys. Chem. A*, 2002, **106**, 1266–1276.
15 N. Di Césare, M. Belletête, M. Leclerc and G. Durocher, *Chem. Phys. Lett.*, 1998, **291**, 487–495.
16 J. Do, J. Huh and E. Kim, *Langmuir*, 2009, **25**, 9405–9412.
17 J. Yoon, S. K. Chae and J. M. Kim, *J. Am. Chem. Soc.*, 2007, **129**, 3038–3039.
18 D. T. McQuade, A. H. Hegedus and T. M. Swager, *J. Am. Chem. Soc.*, 2000, **122**, 12389–12390.
19 J. A. Dean, *Lange's Hand Book of Chemistry*, McGraw Hill Book Company, New York, 1985.
20 (*a*) J. W. Eastman, *Photochem. Photobiol.*, 1967, **6**, 55–72; (*b*) M. J. Adams, J. G. Highfield and G. F. Kirkbright, *Anal. Chem.*, 1977, **49**, 1850–1852.

